Loss of the lupus autoantigen Ro52/Trim21 induces tissue inflammation and systemic autoimmunity by disregulating the IL-23–Th17 pathway

Alexander Espinosa,[1] Valerie Dardalhon,[4] Susanna Brauner,[1] Aurelie Ambrosi,[1] Rowan Higgs,[5] Fransisco J. Quintana,[4] Maria Sjöstrand,[1] Maija-Leena Eloranta,[6] Joan Ní Gabhann,[5] Ola Winqvist,[1] Birgitta Sundelin,[2] Caroline A. Jefferies,[5] Björn Rozell,[3] Vijay K. Kuchroo,[4] and Marie Wahren-Herlenius[1]

[1]Department of Medicine, [2]Department of Oncology and Pathology, and [3]Department of Laboratory Medicine, Karolinska Institute, Stockholm SE-171 77, Sweden
[4]Center for Neurological diseases, Brigham and Women's Hospital, Harvard Medical School, Boston, MA 02115
[5]Molecular and Cellular Therapeutics, Royal College of Surgeons in Ireland, Dublin 2, Ireland
[6]Department of Rheumatology, Uppsala University, Uppsala SE-751 05, Sweden

Ro52/Trim21 is targeted as an autoantigen in systemic lupus erythematosus and Sjögren's syndrome. Polymorphisms in the Ro52 gene have been linked to these autoimmune conditions, but the molecular mechanism by which Ro52 may promote development of systemic autoimmune diseases has not been explored. To address this issue, we generated Ro52-null mice ($Ro52^{-/-}$), which appear phenotypically normal if left unmanipulated. However, $Ro52^{-/-}$ mice develop severe dermatitis extending from the site of tissue injury induced by ear tags. The affected mice further develop several signs of systemic lupus with hypergammaglobulinemia, autoantibodies to DNA, proteinuria, and kidney pathology. Ro52, which was recently identified as an E3 ligase, mediates ubiquitination of several members of the interferon regulatory factor (IRF) family, and the Ro52-deficient mice have an enhanced production of proinflammatory cytokines that are regulated by the IRF transcription factors, including cytokines involved in the Th17 pathway (interleukin [IL] 6, IL-12/IL-23p40, and IL-17). Loss of IL-23/IL-17 by genetic deletion of IL-23/p19 in the $Ro52^{-/-}$ mice conferred protection from skin disease and systemic autoimmunity. These data reveal that the lupus-associated Ro52 protein is an important negative regulator of proinflammatory cytokine production, and they provide a mechanism by which a defective Ro52 function can lead to tissue inflammation and systemic autoimmunity through the IL-23–Th17 pathway.

CORRESPONDENCE
Marie Wahren-Herlenius:
marie.wahren@ki.se

Abbreviations used: ANA, antinuclear antibody; IRF, IFN regulatory factor; SLE, systemic lupus erythematosus; TLR, toll-like receptor.

Systemic lupus erythematosus (SLE) and Sjögren's syndrome are related and partly overlapping autoimmune diseases that share several genetic and phenotypic features. SLE represents a more severe systemic autoimmune condition, but both diseases may involve multiple organs including skin, muscle, joints, and vital internal organs such as kidneys. Both disorders present with activation of type 1 IFN pathways, with increased levels of the cytokines IL-6, IL-12/IL-23p40, and TNF-α (Borchers et al., 2003; Ramanujam and Davidson, 2008), and both conditions have a genetic association with polymorphisms in the IFN regulatory factor (IRF) 5 gene (Sigurdsson et al., 2005; Graham et al., 2006; Nordmark et al., 2009).

Ro52 is a target autoantigen in several systemic autoimmune diseases, including SLE and Sjögren's syndrome, and molecular characterization of Ro52 revealed that it belongs to the TRIM (Tripartite motif) family of proteins (Reymond

A. Espinosa, V. Dardalhon, and S. Brauner contributed equally to this paper.

The Rockefeller University Press $30.00
J. Exp. Med. Vol. 206 No. 8 1661-1671
www.jem.org/cgi/doi/10.1084/jem.20090585

et al., 2001; Hennig et al., 2005, 2008; Ottosson et al., 2006). Like several members of this family, Ro52 has RING-dependent E3 ligase activity (Espinosa et al., 2006) and has been suggested to polyubiquitinate IRF3 and IRF8 (Kong et al., 2007; Higgs et al., 2008). Although genetic polymorphisms in the Ro52 gene have been linked to the development of SLE and Sjögren's syndrome (Frank et al., 1993; Nakken et al., 2001), it has not been addressed how Ro52 regulates cytokine production, tissue inflammation, and development of systemic autoimmunity. To investigate the molecular mechanisms that may link Ro52 to the development of systemic autoimmunity, we generated Ro52-deficient GFP-reporter mice.

RESULTS AND DISCUSSION

Ro52 is an immune-specific gene induced by IFNs

We inserted an IRES-GFP reporter cassette into the Ro52 locus to generate Ro52-deficient mice in which the GFP expression allowed us to track Ro52-expressing cells in vivo (Fig. 1, A–C). Tissue specificity of Ro52 expression has not been investigated systematically, and using GFP as a reporter for Ro52 expression, we observed that Ro52 was predominantly expressed in the lymphoid compartments of spleen, lymph node, and thymus, with little or no expression in nonimmune tissues including liver, pancreas, heart, kidney, and skin (Fig. 1 D and Fig. S1). Some expression was observed in endothelial cells (Fig. S1). Our findings are supported by microarray analysis, showing that Ro52 messenger RNA is predominantly expressed in lymphoid cell populations in both mice and humans (http://biogps.gnf.org). These observations suggest that the primary function of Ro52 may be in the immune system. The vast majority of leukocytes in the bone marrow, thymus, spleen, lymph nodes, and peripheral blood expressed Ro52, as detected by GFP expression, with the highest expression in $CD3^+$ and $CD11b^+GR\text{-}1^+$ cells (Fig. 1 E and not depicted). Using GFP as the reporter, we noted that, as has previously been reported (Rhodes et al., 2002; Strandberg et al., 2008), the expression of Ro52 was induced by IFN-γ and, to a lesser extent, by IFN-α and IFN-β (Fig. 1 F). Other cytokines (TGF-β or TNF-α) did not affect the expression of Ro52 (Fig. 1 F).

$Ro52^{-/-}$ mice were born at a slightly reduced Mendelian ratio ($Ro52^{+/+}$, 27%; $Ro52^{+/-}$, 51%; $Ro52^{-/-}$, 22%; $P = 0.0001$ at $n = 280$, Chi-Square test) without affecting the male/female ratio. However, the $Ro52^{-/-}$ mice that were born appeared normal and had no detectable abnormalities in organ morphology or histology. Specifically, we did not observe any differences in the size or organization in spleen, thymus, and lymph nodes or in subsets of immune cells when comparing young unmanipulated $Ro52^{+/+}$, $Ro52^{+/-}$, and $Ro52^{-/-}$ mice (Figs. S2 and S3). However, splenic $CD3^+$ T cells of $Ro52^{-/-}$ mice had an increased frequency of T cells with an activated phenotype ($CD62L^{low}$; Fig. S3). These data indicate that although there are discreet signs of early activation in splenic T cells in $Ro52^{-/-}$ mice, there is no apparent immune phenotype or other physical abnormalities present in naive unmanipulated Ro52-deficient mice.

Ro52 deficiency leads to tissue inflammation and systemic autoimmunity

Individual mice are routinely identified either by ear punching or by metallic ear tags. After ear tagging with metal clips, no visible tissue reaction, other than transient erythema and swelling, is normally observed. However, 25 wk after application of metal ear tags, >90% of $Ro52^{-/-}$ mice had developed a very severe and progressive dermatitis emanating from the tagged ear, which did not occur in $Ro52^{+/+}$ WT littermates (Fig. 2, A-C). Dermatitis also developed in $Ro52^{+/-}$ mice but was not present in Ro52-deficient mice that had lost their ear tag. Histological analysis of the skin lesions showed epidermal hyperplasia with ulcerations and inflammatory infiltrates consisting primarily of neutrophils (Fig. 2 B). Serum immunoglobulin analysis revealed increased IgG levels in $Ro52^{-/-}$ mice with dermatitis (Fig. 2 D), and the affected mice also developed antinuclear antibodies (ANAs), with specificity for DNA, and autoantibodies to several lupus-associated autoantigens and other autoantigens (Fig. 2 E and Fig. S4). Furthermore, affected mice developed kidney pathology with substantiated mesangium and intraglomerular immunoglobulin depositions, as well as proteinuria, showing impaired renal function (Fig. 2 F). The systemic nature of the inflammation was further supported by the development of splenomegaly and lymphadenopathy in affected mice (Fig. S4 and not depicted). $Ro52^{-/-}$ mice that were not ear tagged did not develop either dermatitis or systemic autoimmunity when observed up to 40 wk of age, suggesting that initial tissue injury induced by physical ear tagging results in uncontrolled tissue inflammation in $Ro52^{-/-}$ mice and, subsequently, leads to development of systemic autoimmunity.

To elucidate the cellular mechanism causing tissue inflammation and systemic autoimmunity in Ro52-deficient mice, we analyzed draining lymph node cells and splenocytes from the affected animals for phenotypic and functional changes. There was a marked expansion of $CD11b^+GR\text{-}1^+$ cells in both spleen and lymph nodes, there was an expansion of $CD19^+$ B cells and $CD3^+$ T cells in the lymph nodes, and the T cells had attained an activated phenotype in the affected mice (Fig. S4). Furthermore, lymph node and spleen cells from affected mice hyperproliferated spontaneously (not depicted) and produced IL-6, IL-12/IL-23p40, IL-21, IL-22, and IL-17 (Fig. 2, G and H), which was further increased upon T cell activation (Fig. 2, G and H). IL-4 and IFN-γ production was not increased in the $Ro52^{-/-}$ mice compared with the $Ro52^{+/+}$ mice (Fig. 2 H). IL-17 in affected mice was produced by $CD4^+$ cells (Fig. 2 I), indicating that Th17 cells are induced in the $Ro52^{-/-}$ mice after skin inflammation. The increased production of IL-17 also begins to explain why dermal lesions are predominantly composed of neutrophils in the $Ro52^{-/-}$ mice, as IL-17 recruits and activates these cells.

High levels of proinflammatory cytokines after immune activation in Ro52-deficient mice

To further study the hyperresponsive immune system of $Ro52^{-/-}$ mice in a more controlled manner, we tested the response in $Ro52^{-/-}$ mice to low doses of the contact-sensitizing

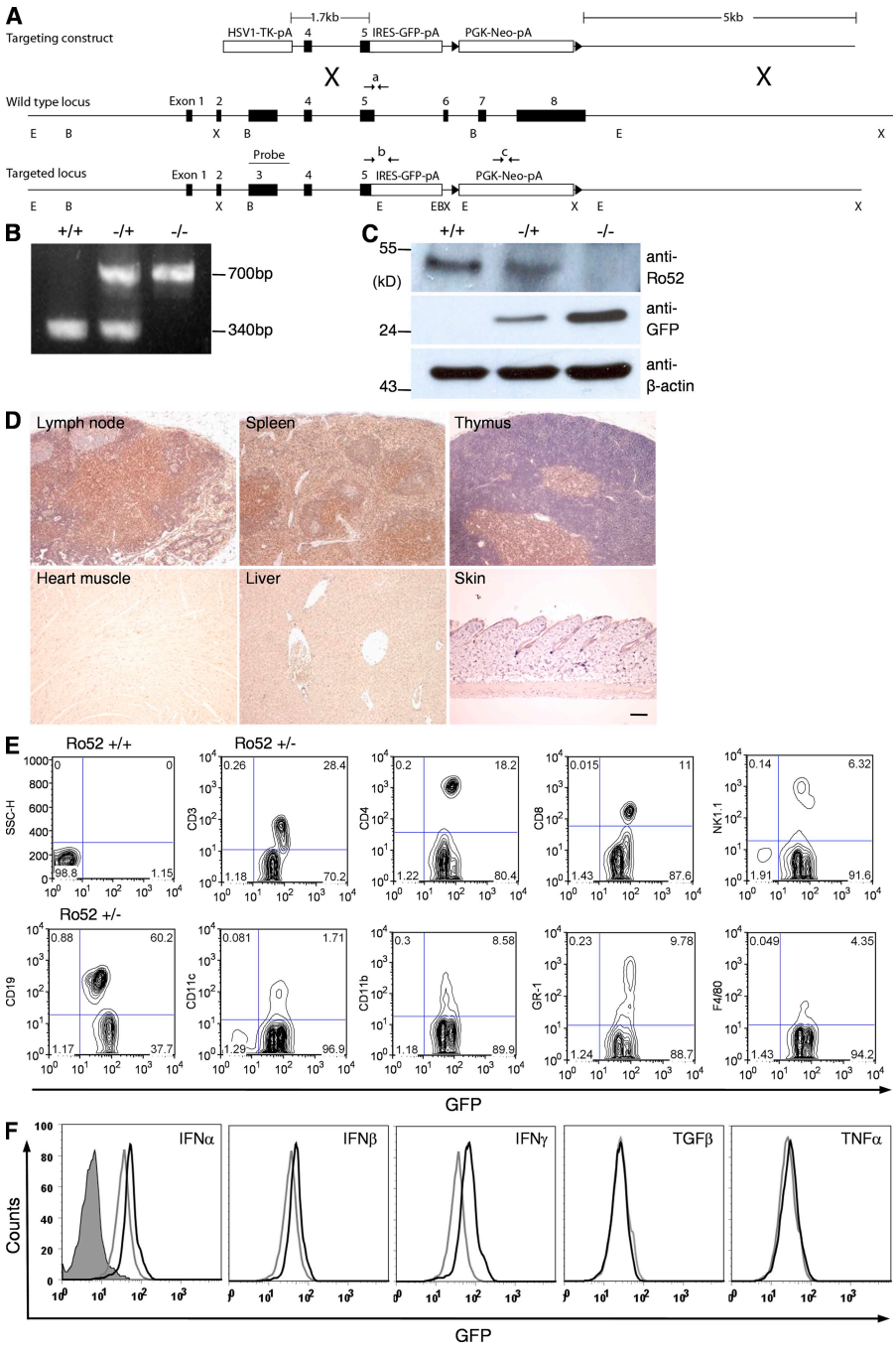

Figure 1. Ro52 is expressed in the immune system and induced by IFNs. (A) Targeting construct for generating Ro52$^{-/-}$ mice. Primer pairs "a" and "b" were used for genotyping WT and targeted allele, respectively. (B) Genotyping PCR for WT (340 bp) and Ro52-null (700 bp) alleles by PCR in Ro52$^{+/+}$, Ro52$^{+/-}$, and Ro52$^{-/-}$ mice. (C) Immunoblotting for Ro52 and GFP expression in splenocyte cell extracts demonstrates loss of Ro52 expression and gain of GFP expression in Ro52$^{+/-}$ and Ro52$^{-/-}$ mice. Data are representative for three independent experiments. (D) Ro52 is specifically expressed in immune tissues as shown by GFP expression (brown) in organ sections (five per organ) from Ro52$^{+/-}$ mice investigated by immunohistochemistry using an anti-GFP antibody. Slides were counterstained with hematoxylin. Data are representative of five independent mice and represent one of two experimental repeats. The original magnification was 10×. Bar, 100 µm. (E) Ro52 is expressed in all major leukocyte populations, as shown by GFP expression in Ro52$^{+/-}$ splenocytes using flow cytometry. The numbers in the quadrants represent the percentage of cells in each quadrant and are representative of 12 mice analyzed in four independent experiments. (F) Ro52 is induced by type I and II IFNs. GFP expression in cells from bone marrow of Ro52$^{+/-}$ mice cultured for 24 h with medium (gray line) or medium + cytokine (black line). Filled histogram represents cells from Ro52$^{+/+}$ mice. Data are representative of three independent experiments.

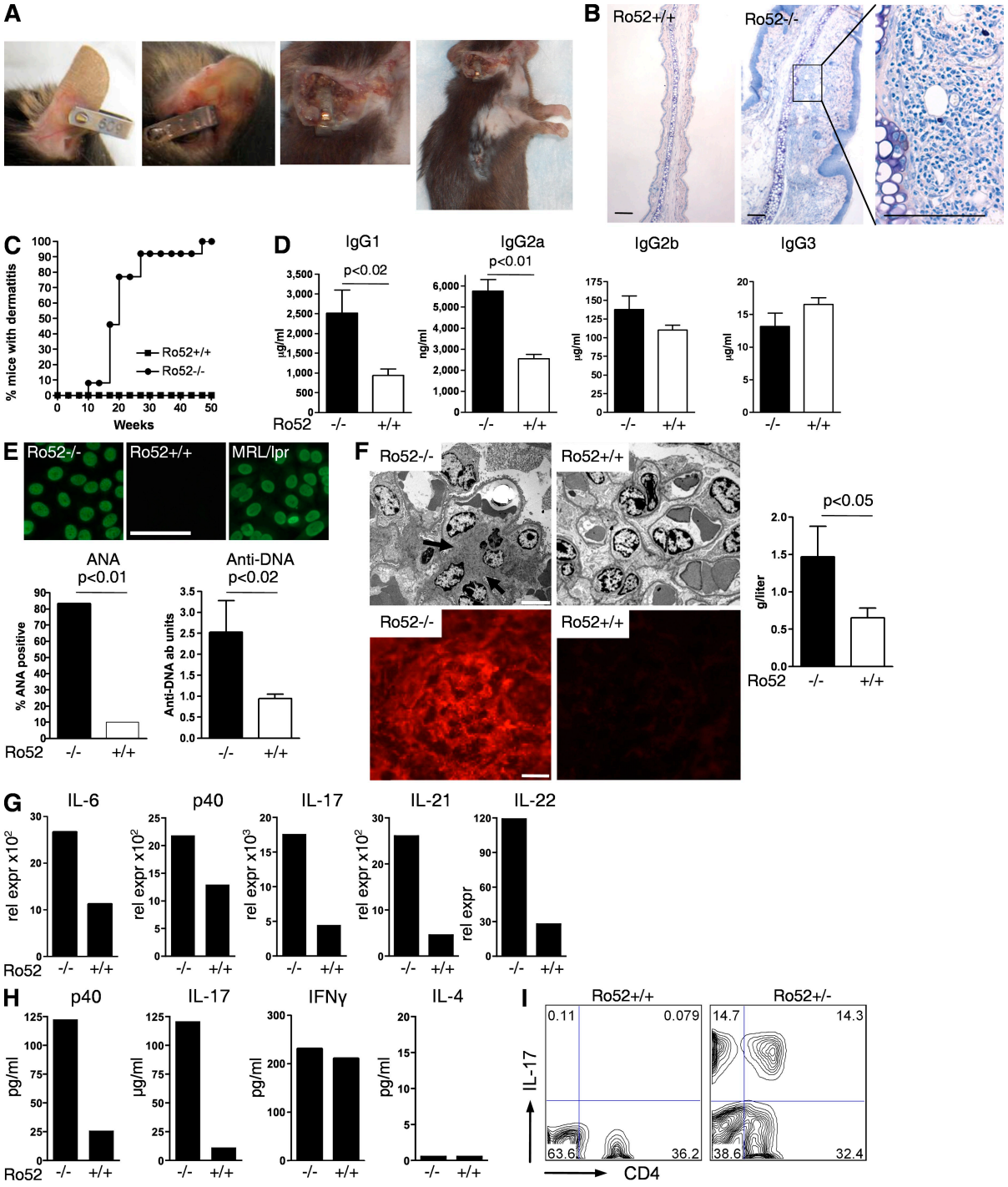

Figure 2. Ro52-deficient mice develop tissue inflammation and systemic autoimmunity. (A) Photographs of the progressive dermatitis developing spontaneously from tissue injury mediated by ear tags in Ro52-deficient mice. Metal tag length, 1 cm. (B) Histology with Toluidine blue staining of ears of tagged $Ro52^{+/+}$ and $Ro52^{-/-}$ mice. Bars, 150 µm. A and B are representative of mice in C. (C) Incidence of dermatitis. 13 independent $Ro52^{-/-}$ mice born during a period of 1.5 yr and their $Ro52^{+/+}$ littermates ($n = 11$) were followed for dermatitis development. Dermatitis developed at different ages but, eventually, in all tagged $Ro52^{-/-}$ mice, whereas none of their littermate controls developed the disease. (D) Serum immunoglobulin levels determined by ELISA in triplicates in $Ro52^{-/-}$ mice with dermatitis ($n = 6$) and $Ro52^{+/+}$ mice ($n = 12$; mean± SEM; Mann-Whitney *U* test). Data represent one of two experimental repeats. (E) $Ro52^{-/-}$ mice with dermatitis develop ANA. Presence of ANA was tested by immunofluorescence of Hep-2 cells and summarized as the percent positive in each group, and anti-DNA antibody levels were measured by ELISA (triplicates) in ANA-positive mice with dermatitis $Ro52^{-/-}$ ($n = 5$) and $Ro52^{+/+}$ ($n = 16$; Mean± SEM; Mann-Whitney *U* test). Data represent one of two experimental repeats. Bar, 75 µm. (F, top) Electron microscopy photographs of renal glomeruli with increased mesangium and immunoglobulin deposition in $Ro52^{-/-}$ mice indicated by arrows. Bar, 2 µm. (F, bottom) Immunofluorescence IgG

agent Oxazolone. Mice lacking Ro52 had a significantly higher contact hypersensitivity to Oxazolone than $Ro52^{+/+}$ mice, as measured by ear thickness (Fig. 3 A), with affected ears showing epidermal hyperplasia and inflammatory infiltrates consisting predominantly of neutrophils (Fig. 3 B). Analysis of lymphoid cell populations in the draining lymph nodes of the $Ro52^{-/-}$ mice treated with Oxazolone showed accumulation of T cells with an activated phenotype (Fig. 3 C) and production of high amounts of the proinflammatory cytokines IL-6, IL-12/IL-23p40, TNF-α, and IL-17 and IL-23R expression after application of Oxazolone (Fig. 3 D). Production of IFN-γ was not different between WT and $Ro52^{-/-}$ mice, and the frequency of $FoxP3^{+}$ cells was not affected (Fig. 3 D). These data demonstrate that a lack of Ro52 leads to dysregulated tissue inflammation with enhanced generation of effector T cells that produce proinflammatory cytokines.

Ro52 is a negative-feedback regulator of proinflammatory cytokine expression

To understand the mechanism by which a deficiency in the Ro52 E3 ligase leads to increased cytokine production and tissue inflammation, we aimed to identify substrates ubiquitinated by Ro52. IRF8 and IRF3 have been suggested as targets for Ro52-mediated ubiquitination (Kong et al., 2007; Higgs et al., 2008). However, as there is a genetic linkage with IRF5 polymorphisms to SLE and Sjögren's syndrome, and proinflammatory cytokines IL-12/IL-23p40, IL-6, and TNF-α, which are increased in $Ro52^{-/-}$ mice, are also regulated by IRF5, we hypothesized that IRF5 may be a substrate for Ro52. Using in vivo ubiquitination assays, we confirmed that IRF3 and IRF8 are polyubiquitinated by Ro52 and, in addition, we observed polyubiquitination of IRF5 by Ro52 (Fig. 4 A). SMAD4, which has structural homology to the IRF proteins, was used as a negative control in our experiments and was not ubiquitinated by Ro52 (Fig. 4 A).

To directly investigate the effects of Ro52 on the transcriptional activity of IRFs, we used a GAL4 one-hybrid luciferase reporter approach. IRF3 and IRF5 fused to GAL4 were tested for their ability to drive luciferase expression from a 4xGAL4-luciferase reporter plasmid upon transfection into 293T cells. Cotransfection with Ro52 substantially decreased IRF3 and IRF5 transcriptional activity in response to toll-like receptor (TLR) 3 or TLR9 signaling induced by polyI:C or CpG stimulation (Fig. 4 B). These findings indicate that a deficiency in Ro52 would lead to increased IRF activity in vivo and persistent production of cytokines induced by IRF3 and 5, such as IL-6, TNF-α, IFN-α, IFN-β, and IL-12/IL-23p40. To investigate the cytokine production in $Ro52^{-/-}$ cells after TLR stimulation, the knockout cells were cultured with TLR agonists including CpG, LPS, polyI:C, and Imiquimod. The stimulation of $Ro52^{-/-}$ splenocytes or bone marrow–derived macrophages resulted in increased expression of cytokines (IL-6, TNF-α, IFN-α, IFN-β, IL-12/IL-23p40, and IL-23p19) compared with $Ro52^{+/+}$ cells (Fig. 4 C and not depicted), confirming that the loss of Ro52 indeed leads to increased expression of many proinflammatory cytokines. Together, our data show that IFNs will induce expression of Ro52 (Fig.1F) and that Ro52, in turn, will suppress expression of the proinflammatory cytokines IL-6, TNF-α, IFN-α, IFN-β, and IL-12/IL-23p40 through ubiquitination of IRF3, 5, and 8. Thus, the cellular role of the IFN-induced Ro52 is to act as a negative-feedback regulator of immune responses and inflammation by suppressing the expression of IRF-induced proinflammatory cytokines.

Disruption of the IL-23–Th17 pathway inhibits tissue inflammation and systemic autoimmunity in $Ro52^{-/-}$ mice

$Ro52^{-/-}$ mice developing dermatitis and systemic autoimmunity produced IL-6 and IL-12/IL-23p40 and had increased levels of Th17 cells in the draining lymph nodes. IL-6 and IL-23 are needed for differentiation and maturation of Th17 cells (Cua et al., 2003; Bettelli et al., 2006), and the IL-23–IL-17 axis appears to be hyperactive in lupus and Sjögren's syndrome (Crispin et al., 2008; Nguyen et al., 2008). We therefore hypothesized that genetic disruption of the IL-23–Th17 pathway rather than the IL-12–IFN-γ pathway would result in inhibition of the tissue inflammation and systemic autoimmunity in $Ro52^{-/-}$ mice. To address this hypothesis, we crossed $Ro52^{-/-}$ mice with $IL\text{-}23p19^{-/-}$ mice to disrupt the IL-23–Th17 pathway. The increased hypersensitivity with dermatitis and inflammatory infiltrates observed in $Ro52^{-/-}$ mice after Oxazolone application was completely reversed in the $Ro52^{-/-}$ mice lacking IL-23p19 chains (Fig. 5, A and B). The enhanced T cell activation observed in $Ro52^{-/-}$ mice was also reversed in the double knockout mice (Fig. 5 C). In addition, the increased expression of IL-23R, IL-12/IL-23p40, IL-17, and RoRγt in the draining lymph nodes of $Ro52^{-/-}$ mice was reversed to baseline levels in the $Ro52^{-/-}p19^{-/-}$ mice (Fig. 5 D). Furthermore, the skin inflammation after ear tagging in the $Ro52^{-/-}$ mice did not develop in ear-tagged

staining of renal glomeruli visualizing deposited IgG (red) and proteinuria (g/liter) in mice with dermatitis $Ro52^{-/-}$ ($n = 7$) and age-matched $Ro52^{+/+}$ mice ($n = 8$; mean± SEM; Mann-Whitney *U* test). Bar, 10 µm. (G) Increased cytokine expression in draining lymph node cells ex vivo from $Ro52^{-/-}$ mice with dermatitis compared with $Ro52^{+/+}$ littermates. Cytokine expression was investigated by quantitative RT-PCR in triplicates and calculated relative to HPRT. Data are representative for five $Ro52^{-/-}$ and five $Ro52^{+/+}$ mice analyzed in five independent experiments and each assay was performed at least twice. (H) Cytokine production in triplicate supernatants was measured by ELISA after culture of cells from draining lymph nodes with 1 µg/ml anti-CD3 (IFN-γ, IL-4, and IL-17) or 1 µg/ml LPS (IL-12/IL-23p40) for 48 h. Data are representative of one $Ro52^{-/-}$ mouse with dermatitis compared with one $Ro52^{+/+}$ mouse in eight independent experiments. Assays were performed at least twice. (I) Cells producing IL-17 were determined by intracellular cytokine staining and flow cytometry of cells from draining lymph nodes after in vitro culture with anti-CD3 for 48 h followed by restimulation with PMA/ionomycin for 4 h. One out of three independent experiments is shown. Numbers in quadrants represent the percentage of cells in each.

$Ro52^{-/-}p19^{-/-}$ in up to 6 mo (30 wk) of observation (Fig. 5, E and F). The $Ro52^{-/-}p19^{-/-}$ mice did not develop ANA or anti-DNA antibodies and did not develop kidney pathology as did the ear-tagged $Ro52^{-/-}$ mice (Fig. 5, G and H). Together, these data demonstrate that abrogating the IL-23–Th17 pathway abolishes tissue inflammation and systemic autoimmunity observed in the Ro52-deficient mice after ear tagging and Oxazolone treatment.

In summary, our studies demonstrate that Ro52 is a key negative regulator of inflammation. Although expressed at a steady-state level, Ro52 is further induced by IFNs (Rhodes et al., 2002; Strandberg et al., 2008), and our data show that Ro52 then acts to control and down-regulate the proinflammatory cytokines IL-6, TNF-α, IFN-α, IFN-β, and IL-12/IL-23p40, thus providing a negative-feedback loop by suppressing IFN-mediated immune activation. Recent studies indicate dual roles for Ro52 (Kim and Ozato, 2009; Yang et al., 2009) and indicate that this E3 ligase may act to sustain IRF3 and IRF8 stability under some conditions but may promote polyubiquitination and degradation of the same transcription factors after TLR- and IFN-mediated activation of cells (Higgs et al., 2008; Kim and Ozato, 2009). Different functions for Ro52 depending on the degree of cellular activation is consistent with our previous observations that Ro52 resides in the cytoplasm in unstimulated cells but translocates into the nucleus upon IFN stimulation (Strandberg et al., 2008) and that Ro52-mediated ubiquitination is supported both by UbcH5 and UbcH6 ubiquitin-conjugating enzymes/E2 ligases that are present in the cytoplasm and nucleus, respectively (Espinosa et al., 2008). In $Ro52^{-/-}$ mice, we observed no obvious phenotype in naive unmanipulated mice, but we did observe a severe unrelenting tissue inflammation after tissue injury, progressing into systemic autoimmunity with several lupus-like features, which was dependent on the IL-23–IL-17 pathway, stressing the importance of Ro52 as a negative regulator of inflammatory responses. Our data begin to build an understanding of how loss or genetic deficiency of Ro52 would result in dysregulation of IFN pathways, a feature which is common to many systemic autoimmune diseases as they present clinically with an "IFN signature" (Baechler et al., 2004; Ronnblom et al., 2006). The Ro52 haploinsufficient mice developed disease at the same frequency and with similar

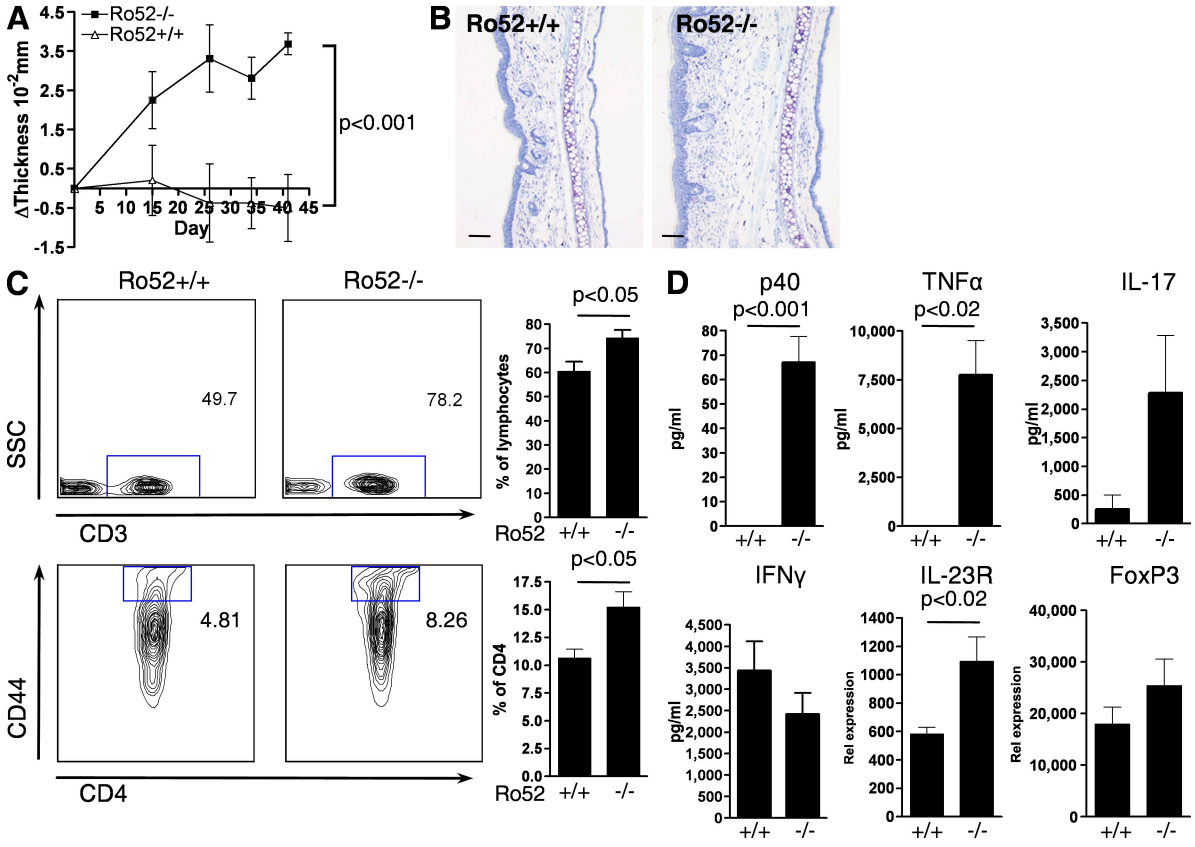

Figure 3. Increased tissue inflammation in $Ro52^{-/-}$ mice. (A) Increased ear thickness in $Ro52^{-/-}$ ($n = 5$) compared with $Ro52^{+/+}$ ($n = 5$) mice after Oxazolone challenge. (ANOVA mixed model). (B) Microphotographs of treated ears. Original magnification, 10×. Bars, 100 µm. (C) Flow cytometry analysis of draining lymph node cells in mice from A. (D) Cytokines in triplicate supernatants of cultures after in vitro stimulation with 1 µg/ml anti-CD3 of cells from draining lymph nodes of five $Ro52^{-/-}$ and five $Ro52^{+/+}$ mice analyzed by ELISA. IL-23R and FoxP3 expression in cells derived from draining lymph nodes of five $Ro52^{-/-}$ and five $Ro52^{+/+}$ mice was analyzed by RT-PCR and calculated relative to HPRT. Data in A–D are representative of three independent experiments. Error bars represent SEM.

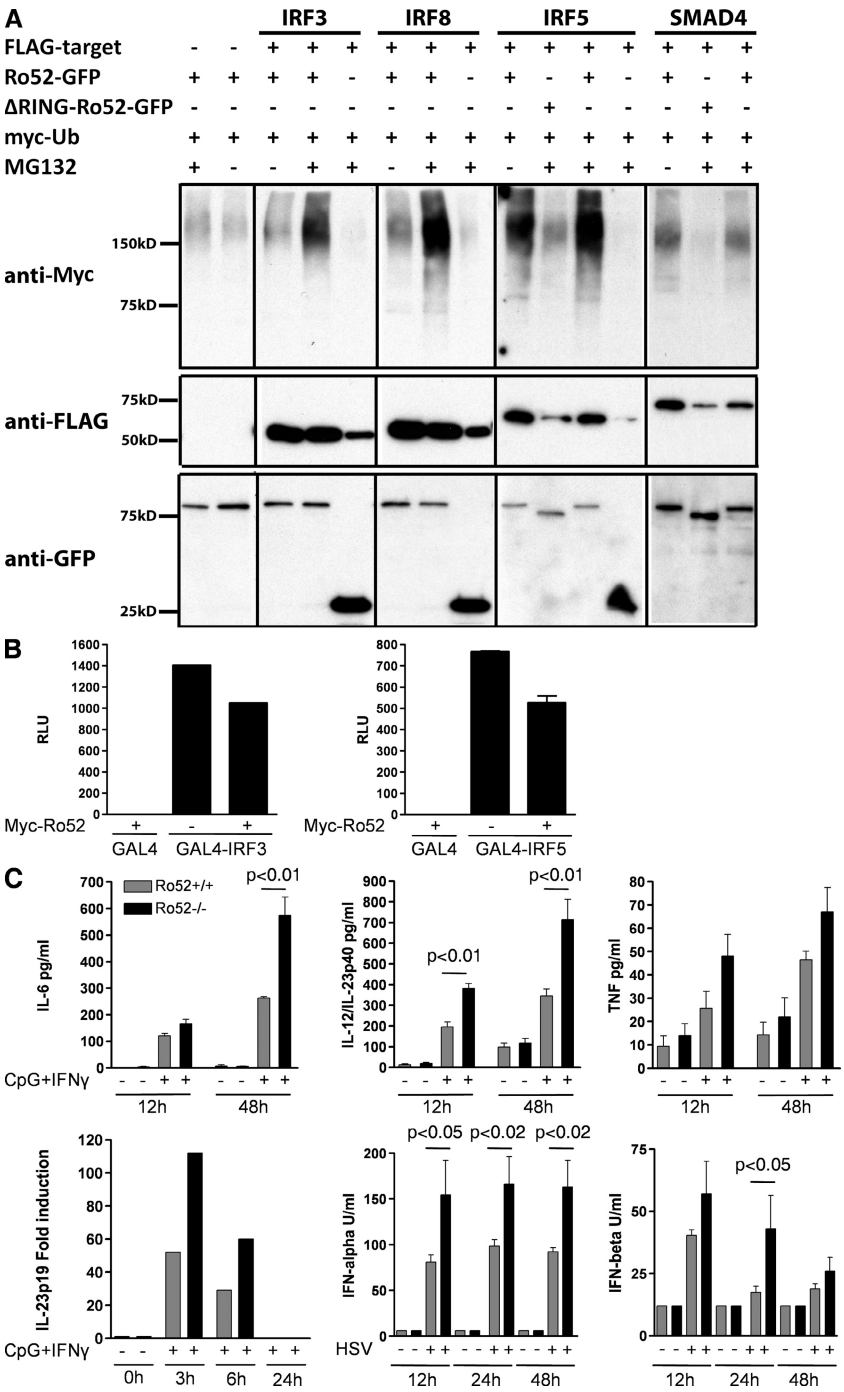

Figure 4. Ro52 inhibits IRF activity and regulates proinflammatory cytokine expression. (A) Immunoblotting of immunoprecipitates from transfected 293T cells show Ro52-mediated polyubiquitination of IRF3, IRF8, and IRF5 but not SMAD4. FLAG-IRFs and Ro52-GFP were detected in whole cell lysates. Data are representative of three independent experiments. Black lines indicate that intervening lanes have been spliced out. (B) The effect of Ro52 on IRF3 and IRF5 activity was investigated in polyI:C-stimulated TLR3 293T transfectants (IRF3) or CpG-stimulated TLR9 293T transfectants (IRF5) using a GAL4 one-hybrid luciferase reporter assay. GAL4-IRF3– and GAL4-IRF5–mediated luciferase expression was diminished by the simultaneous coexpression of Ro52 as compared with an empty vector control (EV), indicating that Ro52 inhibits the activity of IRF3 and IRF5. A representative experiment out of three independent experiments is shown. RLU, relative luciferase units. (C) Increased proinflammatory cytokine production in splenocytes derived from naive Ro52$^{-/-}$ ($n = 5$) compared with Ro52$^{+/+}$ ($n = 5$) mice. Splenocytes were cultured with 2 μg/ml CpG and 100 U/ml IFN-γ or UV-inactivated herpes simplex virus (HSV; 2×10^6 PFU/ml), followed by cytokine measures in supernatants (triplicates) by ELISA or DELFIA (IFN-α and IFN-β). Data are representative of three independent experiments. Error bars represent SEM.

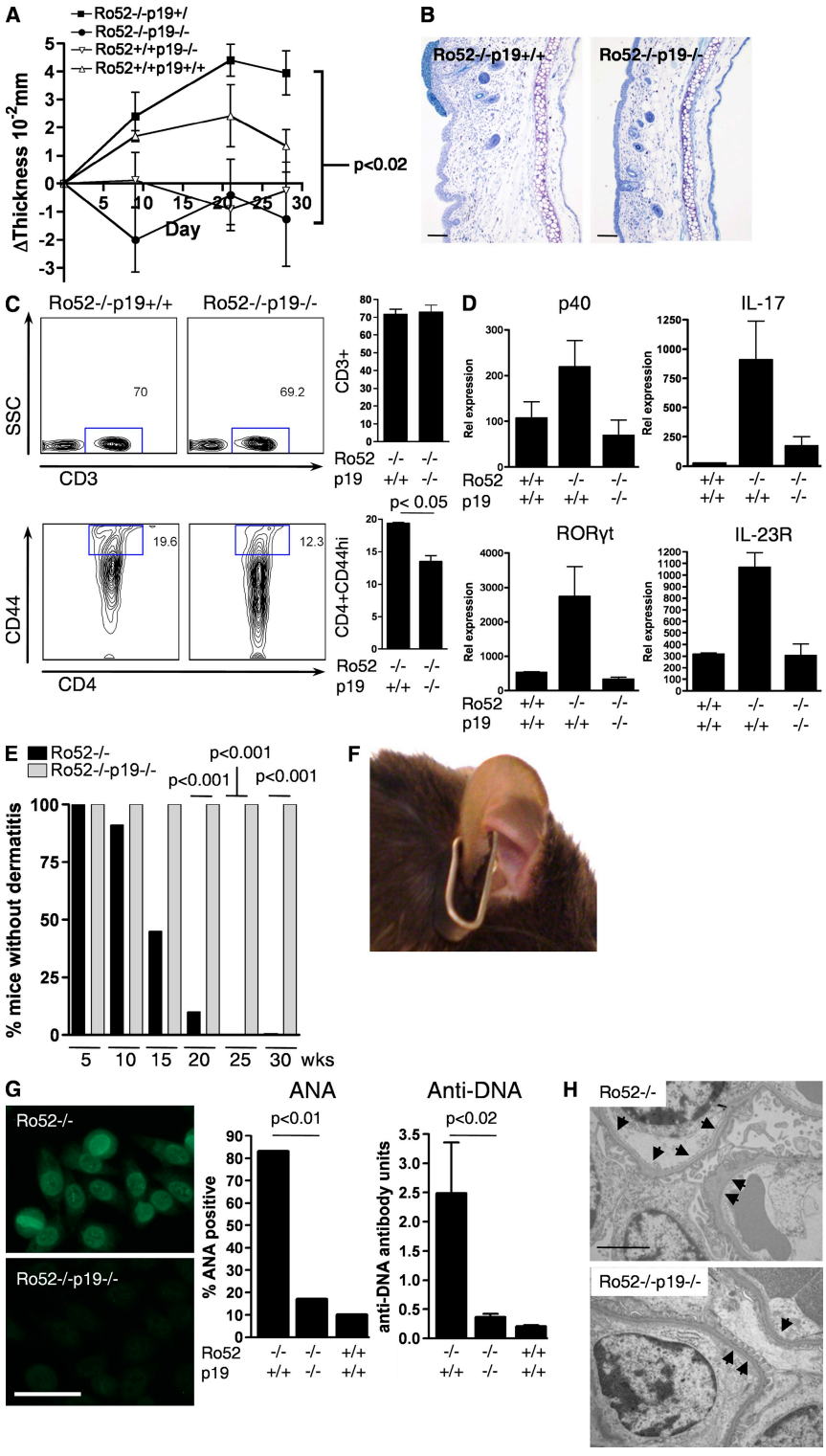

Figure 5. Ro52$^{-/-}$ related tissue inflammation is dependent on the IL-23–IL-17 pathway. (A) Ear thickness after Oxazolone challenge. Ro52$^{-/-}$p19$^{+/+}$, $n = 5$; Ro52$^{-/-}$p19$^{-/-}$, $n = 5$; p19$^{-/-}$Ro52$^{+/+}$, $n = 3$; Ro52$^{+/+}$p19$^{+/+}$, $n = 3$ (ANOVA mixed model). (B) Microphotographs of Oxazolone-treated ears. Ears of all mice in A were analyzed. Original magnification, 10×. Bars, 100 µm. (C) Flow cytometry analysis of draining lymph node cells of Oxazolone-treated mice (Ro52$^{-/-}$p19$^{+/+}$, $n = 5$; Ro52$^{-/-}$p19$^{-/-}$, $n = 5$). (D) Cytokine expression in cells from draining lymph nodes ex vivo measured by RT-PCR with expression relative to HPRT (Ro52$^{-/-}$p19$^{+/+}$, $n = 5$; Ro52$^{-/-}$p19$^{-/-}$, $n = 5$; Ro52$^{+/+}$p19$^{+/+}$, $n = 3$). Data in A–D depicts one out of two representative experiments. Error bars represent SEM. (E) Mice without dermatitis in Ro52$^{-/-}$p19$^{+/+}$ compared with Ro52$^{-/-}$p19$^{-/-}$ mice. Number of mice observed at different ages (Ro52$^{-/-}$p19$^{+/+}$; Ro52$^{-/-}$p19$^{-/-}$): 5 wk (11; 21), 10 wk (11; 18), 15 wk (11; 14), 20 wk (11; 6), 25 wk (11; 5), and 30 wk (11; 4; Fischer's exact test). (F) Ear

phenotypical expression as the mice that completely lacked Ro52, suggesting an important role of Ro52 in regulating immune homeostasis and that even a partial loss of function for this key regulatory protein would result in exaggerated tissue inflammation and systemic autoimmunity. From our data, one would predict that the human genetic linkage to polymorphisms in the Ro52 gene most likely relate to reduction in the level, binding, or function of Ro52 in systemic autoimmune patients.

Although the role of IL-17 and the Th17 pathway in lupus and Sjögren's syndrome is only beginning to be explored, several studies implicate a role for Th17 effector cells also in these autoimmune conditions (Crispin et al., 2008; Nguyen et al., 2008; Sakai et al., 2008; Wong et al., 2008). Furthermore, our data suggest that loss of IL-17 also suppresses development of exaggerated skin inflammation in Ro52$^{-/-}$ animals. Together, the present data link Ro52, an E3 ligase which targets many transcription factors in the IFN pathway, to disregulated proinflammatory cytokine production and to the development of tissue specific inflammation and systemic autoimmunity.

MATERIALS AND METHODS

Generation of Ro52$^{-/-}$ mice. Ro52$^{-/-}$ mice were generated using standard gene targeting techniques. In brief, a short (1.7 kb) and a long (5 kb) arm were PCR cloned from the C57BL/6J BAC clone RP23-311N6 using the following primers: short arm, forward, 5′-ATCGATTGCAGAGGCAAAGCCATGGGAAAG-3′, and reverse, 5′-ATCGATTCCTCCTCTCCAGCTCTGAGATCA-3′; and long arm, forward, 5′-GTCGACAGGCTACAACAGCTGTGCTCAGA-3′, and reverse, 5′-GCGGCCGCACCCTGGCCTTGATTTCTAACAG-3′. They were then ligated into the gene targeting cassette vector pKS-TK-NeoloxP-IRES-GFP. The C57BL/6-derived embryonic stem cell line V26.2 was used for homologous recombination, and targeted embryonic stem cell clones were identified by Southern blotting and injected into BALB/c embryos. Chimeras carrying the target allele were bred to C57BL/6J mice. Ro52$^{-/-}$p19$^{-/-}$ mice were generated by intercrossing Ro52$^{-/-}$ and p19$^{-/-}$ mice obtained from the Mutant mouse Regional Resource Center (www.mmrrc.org). The study was approved by the Ethical Review Committee North, Stockholm County and Standing Committee on Animals at Harvard Medical School.

Histochemistry and electron microscopy. Organs were fixed in 4% paraformaldehyde for 24 h, embedded in paraffin, and 4–5-µm sections stained with hematoxylin/eosin or Toluidine blue or were used in immunohistochemistry with rabbit polyclonal anti-GFP (Invitrogen), rat monoclonal anti-CD3 (clone SP7; Thermo Fisher Scientific), or rat monoclonal anti-B220 (clone RA3-6B2; BD). Antigen retrieval was performed using Retriever 2100 (PickCell Laboratories). For electron microscopy, small pieces of kidneys were further fixed in 2.5% glutaraldehyde and postfixed in 1% OsO_4 plus 1% potassium ferrocyanide, followed by staining with 0.5% uranyl acetate. After dehydration, specimens were embedded in epoxy resin (agar 100) and cured by heat. 50-nm sections were contrasted with lead citrate and uranyl acetate and examined with an electron microscope (912AB; Carl Zeiss, Inc.) equipped with a MegaView III camera (Olympus) for digital image capture. Immunofluorescence staining of kidneys was performed on 7-µm paraformaldehyde-fixed sections of snap-frozen organs with an Alexa Flour 594–conjugated donkey anti–mouse IgG (Invitrogen).

Cell isolation and flow cytometry. Single cell suspensions were prepared from lymphoid organs and cells blocked in Fc block (BD) for 30 min before staining by fluorophore-conjugated antibodies (BD). For intracellular cytokine staining, cells stimulated in vitro with soluble anti-CD3 were restimulated for 4 h with 50 ng/ml PMA (Sigma-Aldrich), 1 µg/ml ionomycin (Sigma-Aldrich), and 1 µl/ml GolgiStop (BD), followed by surface marker and intracellular cytokine staining according to the manufacturer's instructions. Cells were analyzed on a flow cytometer (BD).

Serologic and proteinuria analyses. Immunoglobulin isotype serum leves were analyzed using the SBA Clonotyping System/AP kit (Southern-Biotech), ANA by Hep-2 slides (Immuno Concepts), and anti-DNA antibodies, as previously described (Wermeling et al., 2007), in ELISA using plates coated with methylated bovine serum albumin and activated calf thymus DNA (Sigma-Aldrich). Lupus autoantigen microarrays were generated and used, as previously described, with 41 autoantigens spotted in replicates of six (Wu et al., 2008). Sera were diluted 1:50–1:100 in the assays. Proteinuria was detected using Multistix 5 (Bayer).

Cytokine analysis by ELISA and quantitative RT-PCR. Culture supernatants were collected after stimulation, as defined in each experiment, to assess cytokine production by ELISA or cytometric bead array (R&D Systems; BD). IFN-α was quantified by dissociation-enhanced lanthanide fluoroimmunoassay as previously described (Strandberg et al., 2008). RNA was extracted with RNeasy columns (QIAGEN) from cells ex vivo and analyzed by quantitative RT-PCR according to the manufacturer's instructions (Applied Biosystems) and expression related to HPRT.

Oxazolone provocation. Oxazolone (4-ethozymethylene-2-phenyl-2-oxazolin-5-one) provocation was performed using the ear swelling test as described in Yokozeki et al. (2000). Mice were sensitized on shaved back skin with 150 µl of 0.3% Oxazolone (Sigma-Aldrich) dissolved in acetone/olive oil (4:1) applied on two consecutive days. 5 d later, the ears were challenged with 50 µl of a 0.1% Oxazolone solution on one ear and with the vehicle on the other. This was repeated on three consecutive days, and ear swelling was measured by a micrometer (Kroeplin). The whole procedure was repeated up to four times. Change in thickness was calculated by subtracting swelling caused by the vehicle.

Ubiquitination assays. 293T cells were transfected with 500 ng FLAG-IRF or FLAG-SMAD4, 500 ng Ro52-GFP, and 500 ng Myc-ubiquitin. The SMAD4 plasmid was a gift from C.-H. Heldin (Uppsala University, Uppsala, Sweden). 10 µM MG132 was added 28 h after transfection and cells were harvested 6 h later. Cells were lysed in immunoprecipitation buffer and, after clearing of the lysate, FLAG-M2-agarose beads (Sigma-Aldrich) were added, followed by incubation for 2 h. After washing, FLAG-IRFs were eluted with FLAG peptide (Sigma-Aldrich) and separated by SDS-PAGE, and ubiquitinated FLAG-IRFs were detected by immunoblotting against Myc (Santa Cruz Biotechnology, Inc.). FLAG-IRFs and GFP-Ro52 were detected in whole cell lysates by immunoblotting against FLAG (Sigma-Aldrich) and GFP (Sigma-Aldrich).

Luciferase assays. For measurement of IRF activity, 10^5 293T cells were transfected in triplicates in 24-well plates using Fugene HD (Roche). Each well was transfected with 20 ng GAL4-IRF, 20 ng MycRo52 or empty Myc vector, 20 ng pRL-TK-*Renilla*, 20 ng pcDNA3.1-TLR9 or pFLAG-CMV1-TLR3 (gift from R. Medzhitov, Yale University, New Haven, CT; plasmids 13084 and 13091, respectively; Addgene), and 50 ng GAL4 reporter plasmid MH100-luc. After 16 h, cells were harvested and prepared for the reporter

with tag in Ro52$^{-/-}$p19$^{-/-}$ mouse showing no inflammation or dermatitis. Data are representative of mice in E. Metal tag length, 1 cm. (G) ANA analysis tested by immunofluorescence of Hep-2 cells and summarized as the percent positive in each group, and anti-DNA antibody levels measured by ELISA (triplicates) in Ro52$^{-/-}$ p19$^{+/+}$ (n = 7), Ro52$^{-/-}$p19$^{-/-}$ (n = 10), and Ro52$^{+/+}$p19$^{+/+}$ (n = 7; mean ± SEM; Mann-Whitney U test). Bar, 50 µm. (H) Electron microscopy image of kidneys depicting reversal of pathological changes in Ro52$^{-/-}$p19$^{-/-}$ mice (arrows). All mice in A were analyzed. Bar, 2 µm.

assay (Dual-Luciferase Reporter Assay system; Promega). Firefly luciferase luminescence was normalized to *Renilla* luminescence and used as a measure of IRF activity. Results are shown relative to transfections in which GAL4 was not fused to any IRF.

Statistical analysis. Data are expressed as mean ± SEM. Analysis of nonparametric data between groups was performed with a Mann-Whitney *U* test. Analysis, including repeated measures, was performed with an ANOVA mixed model, and a Fischer's exact test was used for analysis of frequencies between groups in small samples.

Online supplemental material. Fig. S1 shows expression of GFP as a reporter for Ro52. Fig. S2 shows lymphoid organization in $Ro52^{+/+}$, $Ro52^{+/-}$, and $Ro52^{-/-}$ mice. Fig. S3 shows leukocyte cell populations in naive mice. Fig. S4 shows autoantibody reactivity and splenomegaly in $Ro52^{-/-}$ mice. Online supplemental material is available at http://www.jem.org/cgi/content/full/jem.20090585/DC1.

We thank Nora Ramirez, Vijole Dzikaite, and Ann Trönnberg for skillful technical assistance, Mohamed Oukka for targeting vector design, Henrik Källberg for statistical analyses, and Professor Carl-Henrik Heldin (Uppsala University, Uppsala, Sweden) for the gift of the SMAD4 plasmid.

This work was supported by grants from the Swedish Research Council, the Swedish Foundation for Strategic Research, the Stockholm County Council, King Gustaf the Vth 80-year foundation, the Göran Gustafsson Foundation, the Torsten and Ragnar Söderberg Foundation, the Heart-Lung Foundation, Science Foundation Ireland, and the Swedish Rheumatism Association.

The authors have no conflicting financial interests.

Submitted: 16 March 2009
Accepted: 22 June 2009

REFERENCES

Baechler, E.C., P.K. Gregersen, and T.W. Behrens. 2004. The emerging role of interferon in human systemic lupus erythematosus. *Curr. Opin. Immunol.* 16:801–807.

Bettelli, E., Y. Carrier, W. Gao, T. Korn, T.B. Strom, M. Oukka, H.L. Weiner, and V.K. Kuchroo. 2006. Reciprocal developmental pathways for the generation of pathogenic effector TH17 and regulatory T cells. *Nature.* 441:235–238.

Borchers, A.T., S.M. Naguwa, C.L. Keen, and M.E. Gershwin. 2003. Immunopathogenesis of Sjogren's syndrome. *Clin. Rev. Allergy Immunol.* 25:89–104.

Crispin, J.C., M. Oukka, G. Bayliss, R.A. Cohen, C.A. Van Beek, I.E. Stillman, V.C. Kyttaris, Y.T. Juang, and G.C. Tsokos. 2008. Expanded double negative T cells in patients with systemic lupus erythematosus produce IL-17 and infiltrate the kidneys. *J. Immunol.* 181:8761–8766.

Cua, D.J., J. Sherlock, Y. Chen, C.A. Murphy, B. Joyce, B. Seymour, L. Lucian, W. To, S. Kwan, T. Churakova, et al. 2003. Interleukin-23 rather than interleukin-12 is the critical cytokine for autoimmune inflammation of the brain. *Nature.* 421:744–748.

Espinosa, A., W. Zhou, M. Ek, M. Hedlund, S. Brauner, K. Popovic, L. Horvath, T. Wallerskog, M. Oukka, F. Nyberg, et al. 2006. The Sjogren's syndrome-associated autoantigen Ro52 is an E3 ligase that regulates proliferation and cell death. *J. Immunol.* 176:6277–6285.

Espinosa, A., V. Oke, A. Elfving, F. Nyberg, R. Covacu, and M. Wahren-Herlenius. 2008. The autoantigen Ro52 is an E3 ligase resident in the cytoplasm but enters the nucleus upon cellular exposure to nitric oxide. *Exp. Cell Res.* 314:3605–3613.

Frank, M.B., K. Itoh, A. Fujisaku, P. Pontarotti, M.G. Mattei, and B.R. Neas. 1993. The mapping of the human 52-kD Ro/SSA autoantigen gene to human chromosome 11, and its polymorphisms. *Am. J. Hum. Genet.* 52:183–191.

Graham, R.R., S.V. Kozyrev, E.C. Baechler, M.V. Reddy, R.M. Plenge, J.W. Bauer, W.A. Ortmann, T. Koeuth, M.F. Gonzalez Escribano, B. Pons-Estel, et al. 2006. A common haplotype of interferon regulatory factor 5 (IRF5) regulates splicing and expression and is associated with increased risk of systemic lupus erythematosus. *Nat. Genet.* 38:550–555.

Hennig, J., L. Ottosson, C. Andresen, L. Horvath, V.K. Kuchroo, K. Broo, M. Wahren-Herlenius, and M. Sunnerhagen. 2005. Structural organization and Zn2+-dependent subdomain interactions involving autoantigenic epitopes in the Ring-B-box-coiled-coil (RBCC) region of Ro52. *J. Biol. Chem.* 280:33250–33261.

Hennig, J., A. Bresell, M. Sandberg, K.D. Hennig, M. Wahren-Herlenius, B. Persson, and M. Sunnerhagen. 2008. The fellowship of the RING: the RING-B-box linker region interacts with the RING in TRIM21/Ro52, contains a native autoantigenic epitope in Sjogren syndrome, and is an integral and conserved region in TRIM proteins. *J. Mol. Biol.* 377:431–449.

Higgs, R., J. Ni Gabhann, N. Ben Larbi, E.P. Breen, K.A. Fitzgerald, and C.A. Jefferies. 2008. The E3 ubiquitin ligase Ro52 negatively regulates IFN-beta production post-pathogen recognition by polyubiquitin-mediated degradation of IRF3. *J. Immunol.* 181:1780–1786.

Kim, J.Y., and K. Ozato. 2009. The sequestosome 1/p62 attenuates cytokine gene expression in activated macrophages by inhibiting IFN regulatory factor 8 and TNF receptor-associated factor 6/NF-kappaB activity. *J. Immunol.* 182:2131–2140.

Kong, H.J., D.E. Anderson, C.H. Lee, M.K. Jang, T. Tamura, P. Tailor, H.K. Cho, J. Cheong, H. Xiong, H.C. Morse III, and K. Ozato. 2007. Cutting edge: autoantigen Ro52 is an interferon inducible E3 ligase that ubiquitinates IRF-8 and enhances cytokine expression in macrophages. *J. Immunol.* 179:26–30.

Nakken, B., R. Jonsson, and A.I. Bolstad. 2001. Polymorphisms of the Ro52 gene associated with anti-Ro 52-kd autoantibodies in patients with primary Sjogren's syndrome. *Arthritis Rheum.* 44:638–646.

Nguyen, C.Q., M.H. Hu, Y. Li, C. Stewart, and A.B. Peck. 2008. Salivary gland tissue expression of interleukin-23 and interleukin-17 in Sjogren's syndrome: findings in humans and mice. *Arthritis Rheum.* 58:734–743.

Nordmark, G., G. Kristjansdottir, E. Theander, P. Eriksson, J.G. Brun, C. Wang, L. Padyukov, L. Truedsson, G. Alm, M.L. Eloranta, et al. 2009. Additive effects of the major risk alleles of IRF5 and STAT4 in primary Sjogren's syndrome. *Genes Immun.* 10:68–76.

Ottosson, L., J. Hennig, A. Espinosa, S. Brauner, M. Wahren-Herlenius, and M. Sunnerhagen. 2006. Structural, functional and immunologic characterization of folded subdomains in the Ro52 protein targeted in Sjogren's syndrome. *Mol. Immunol.* 43:588–598.

Ramanujam, M., and A. Davidson. 2008. Targeting of the immune system in systemic lupus erythematosus. *Expert Rev. Mol. Med.* 10:e2.

Reymond, A., G. Meroni, A. Fantozzi, G. Merla, S. Cairo, L. Luzi, D. Riganelli, E. Zanaria, S. Messali, S. Cainarca, et al. 2001. The tripartite motif family identifies cell compartments. *EMBO J.* 20:2140–2151.

Rhodes, D.A., G. Ihrke, A.T. Reinicke, G. Malcherek, M. Towey, D.A. Isenberg, and J. Trowsdale. 2002. The 52 000 MW Ro/SS-A autoantigen in Sjogren's syndrome/systemic lupus erythematosus (Ro52) is an interferon-gamma inducible tripartite motif protein associated with membrane proximal structures. *Immunology.* 106:246–256.

Ronnblom, L., M.L. Eloranta, and G.V. Alm. 2006. The type I interferon system in systemic lupus erythematosus. *Arthritis Rheum.* 54:408–420.

Sakai, A., Y. Sugawara, T. Kuroishi, T. Sasano, and S. Sugawara. 2008. Identification of IL-18 and Th17 cells in salivary glands of patients with Sjogren's syndrome, and amplification of IL-17-mediated secretion of inflammatory cytokines from salivary gland cells by IL-18. *J. Immunol.* 181:2898–2906.

Sigurdsson, S., G. Nordmark, H.H. Goring, K. Lindroos, A.C. Wiman, G. Sturfelt, A. Jonsen, S. Rantapaa-Dahlqvist, B. Moller, J. Kere, et al. 2005. Polymorphisms in the tyrosine kinase 2 and interferon regulatory factor 5 genes are associated with systemic lupus erythematosus. *Am. J. Hum. Genet.* 76:528–537.

Strandberg, L., A. Ambrosi, A. Espinosa, L. Ottosson, M.L. Eloranta, W. Zhou, A. Elfving, E. Greenfield, V.K. Kuchroo, and M. Wahren-Herlenius. 2008. Interferon-alpha induces up-regulation and nuclear translocation of the Ro52 autoantigen as detected by a panel of novel Ro52-specific monoclonal antibodies. *J. Clin. Immunol.* 28:220–231.

Wermeling, F., Y. Chen, T. Pikkarainen, A. Scheynius, O. Winqvist, S. Izui, J.V. Ravetch, K. Tryggvason, and M.C. Karlsson. 2007. Class A scavenger receptors regulate tolerance against apoptotic cells, and autoantibodies against these receptors are predictive of systemic lupus. *J. Exp. Med.* 204:2259–2265.

Wong, C.K., L.C. Lit, L.S. Tam, E.K. Li, P.T. Wong, and C.W. Lam. 2008. Hyperproduction of IL-23 and IL-17 in patients with systemic lupus erythematosus: implications for Th17-mediated inflammation in auto-immunity. *Clin. Immunol.* 127:385–393.

Wu, H.Y., F.J. Quintana, and H.L. Weiner. 2008. Nasal anti-CD3 antibody ameliorates lupus by inducing an IL-10-secreting CD4+ CD25- LAP+ regulatory T cell and is associated with down-regulation of IL-17+ CD4+ ICOS+ CXCR5+ follicular helper T cells. *J. Immunol.* 181:6038–6050.

Yang, K., H.X. Shi, X.Y. Liu, Y.F. Shan, B. Wei, S. Chen, and C. Wang. 2009. TRIM21 is essential to sustain IFN regulatory factor 3 activation during antiviral response. *J. Immunol.* 182:3782–3792.

Yokozeki, H., M. Ghoreishi, S. Takagawa, K. Takayama, T. Satoh, I. Katayama, K. Takeda, S. Akira, and K. Nishioka. 2000. Signal transducer and activator of transcription 6 is essential in the induction of contact hypersensitivity. *J. Exp. Med.* 191:995–1004.